Received 1 April 2024; revised 5 May 2024; accepted 21 May 2024. Date of publication 27 May 2024; date of current version 18 June 2024.

Digital Object Identifier 10.1109/OJCOMS.2024.3406340

Extending RIS Life Span for Reliable Communication Under Hardware Ageing Effects

ATIQUZZAMAN MONDAL [1], SHYAMAL GHOSH [2] (Member, IEEE), KESHAV SINGH [3] (Member, IEEE), SUDIP BISWAS [1] (Member, IEEE), AND TRUNG Q. DUONG [4,5] (Fellow, IEEE)

[1]Department of Electrical Communication Engineering, Indian Institute of Information Technology Guwahati, Guwahati 781015, India

[2]Department of Data Science, Indian Institute of Science Education and Research Thiruvananthapuram, Thiruvananthapuram 695551, India

[3]Institute of Communications Engineering, National Sun Yat-sen University, Kaohsiung 80424, Taiwan

[4]Faculty of Engineering and Applied Science, Memorial University, St. John's, NL A1C 5S7, Canada

[5]School of Electronics, Electrical Engineering and Computer Science, Queen's University Belfast, BT7 1NN Belfast, U.K.

CORRESPONDING AUTHOR: K. SINGH (e-mail: keshav.singh@mail.nsysu.edu.tw).

The work of Atiquzzaman Mondal and Sudip Biswas was supported by the Science and Engineering Research Board (SERB), India, under Grant IMC/2020/000015 and Grant CRG/2023/003524. The work of Keshav Singh was supported in part by the National Science and Technology Council of Taiwan under Grant NSTC 112-2218-E-110-004, and in part by the Sixth Generation Communication and Sensing Research Center funded by the Higher Education SPROUT Project, the Ministry of Education of Taiwan. The work of Trung Q. Duong was supported in part by the Canada Excellence Research Chair (CERC) Program under Grant CERC-2022-00109.

ABSTRACT In this paper, we address the critical aspect of hardware ageing effects in reconfigurable intelligent surfaces (RISs), whereby the problem of extending the RIS's life cycle under the impact of non-residual stochastic hardware impairment is considered. Through the replication of the RIS hardware and diverse wireless environments within a statistical simulation environment, we formulate an electronic maintenance framework (EMF) for RIS, where we incorporate non-residual impairments through stochastic modeling and determine the electronic reliability of the system. Accordingly, we derive optimal analytical solutions within the EMF to determine whether systematic maintenance of the RIS hardware should be done immediately or postponed in order to extend the expected life cycle of the RIS system. Furthermore, for the scenario with imperfect maintenance of the RIS-aided system, a reliable communication framework (RCF) is also introduced with residual impairments to assess the error probability of the RIS-aided communication. The RCF is established by deriving the distribution of the received signal-to-interference-plus-noise ratio in the presence of residual hardware impairment arising due to imperfect maintenance of the RIS system. Extensive numerical examples are provided to elucidate the derived solutions and illustrate the reliability performance of the proposed framework under hardware impairments.

INDEX TERMS Industrial informatics and communication, electronic maintenance, industrial Internet-of-Things, reliability, reconfigurable intelligent surfaces, hardware impairment.

I. INTRODUCTION

RECONFIGURABLE intelligent surface (RIS) is a type of metasurface [1], [2] that can dynamically modify the propagation of electromagnetic waves [3], [4]. RISs have been identified as a key enabling technology for sixth-generation (6G) wireless communications and Industry 5.0 [5], [6]. RIS technology can enhance the capabilities of industrial Internet of Things (IIoT) devices by improving connectivity and reducing latency, which is crucial for real-time monitoring and automation in industries [7]. RIS can also assist multi-target sensing in IIoT networks [8], particularly precise target localization and environment mapping within an industrial setting. By dynamically modifying the propagation of electromagnetic waves, a RIS can adapt to changing environmental conditions and optimize the wireless channel for maximum throughput and energy efficiency

[9], [10], and efficient localization and environment mapping [11], [12]. In particular, RIS can smartly control the propagation environment, which is useful in factories or industrial plants where metal structures often cause signal reflection and scattering, leading to communication and sensing dead zones. Furthermore, in industrial environments where numerous sensors and devices are connected wirelessly, RIS can help reduce the overall energy consumption of the system. These are achieved by embedding the RIS with electronically controlled elements (ECEs), such as varactors or micro-electro-mechanical systems (MEMS) switches, which can change the characteristics of the surface on demand [13], [14]. The potential benefits of a RIS-assisted wireless communications have generated significant interest from industry and academia, and research efforts are currently underway to develop practical RIS solutions for next-generation IIoT networks.

In industrial settings, consistent and reliable communication is vital. A communication link's reliability is dependent on the level of noise at the receiver of the communication system. The noise in the system is due to the inherent wireless propagation environment as well as hardware impairments of the communication devices. While RISs can provide a plethora of advantages in modifying the wireless propagation environment, their hardware reliability is a critical aspect of their practical applications in 6G communications. Due to their sub-wavelength structure, metasurfaces are vulnerable to environmental factors [15], [16] such as temperature, humidity, and mechanical stress, which gives rise to continuous hardware impairments that can alter the electromagnetic properties of RISs and reduce their lifetime. Increasing the life cycle of RISs is an essential aspect, as a failure of the system in mission-critical ultra-reliable wireless applications can cost more than the planned maintenance. Sometimes, the structure needs to be replaced if maintenance is not done on time. Furthermore, extending the life cycle of the RIS can be an essential strategy for reducing e-waste, thus ameliorating its negative impact on the environment. As the use of RIS in IIoT networks is expected to proliferate and become a more significant source of greenhouse gas emissions, initiatives to promote the extension of the life span of the ECEs of RISs are critical in addressing this global challenge. Accordingly, monitoring the linearly increasing hardware impairment of RISs and extending their lifetime can significantly lower CO_2 emissions associated with the production and disposal of metasurfaces throughout the industrial process.

Typically, failures in systems are categorized as sudden or gradual based on the failure mechanisms and the available information, with gradual failures resulting from an impairment process reaching a specific threshold [17], [18], [19]. This prior information on impairment is crucial for achieving perfect repair or maintenance of RIS-aided wireless networks. However, the harsh and dynamic wireless environments of the real world and the extremely dense deployment of RISs make analyzing such networks in real-time difficult. While the ongoing development of RIS technology focuses on enabling high-capacity [20], energy-efficient [20], [21], and secure [22] wireless networks, a gap exists in studies addressing the reliability of communication networks during their physical operation. Furthermore, a few studies that do focus on hardware impairment in RIS-aided networks consider residual impairment factors such as phase imperfections and transceiver noise [23], [24] only. Other studies, such as [25] and [26] focus on the analysis of enterprise data-center networks and virtual network functions, respectively. This work addresses the existing gap by concentrating on the electronic reliability of RIS-aided communication systems. We introduce non-residual stochastic RIS hardware impairments[1] as a method to comprehend the life cycle of RISs, which encompasses the period from their deployment in communication networks to the point at which performance degradation due to hardware ageing impacts their operational effectiveness. Key aspects of the RIS's life cycle include:

- Initiation: The point of deployment where RIS begins its operational life, configured to enhance communication networks.
- Operational Peak: The period during which RIS operates at optimal efficiency, providing maximum communication enhancements without significant degradation.
- Degradation Onset: The phase where signs of hardware ageing, such as reduced signal reflection or absorption capabilities, begin to manifest, gradually affecting performance.
- Critical Threshold: A defined limit beyond which the performance degradation of RIS significantly impairs communication quality, marking a need for maintenance or replacement.
- End-of-Life: The stage where RIS can no longer be feasibly maintained to meet operational standards and must be decommissioned or replaced.

In contrast to traditional residual impairment factors, the impact of stochastic impairments on RIS performance is intricately linked to its service management in terms of both run-time and longevity. This aspect has not been explored in the existing RIS literature. Consequently, we propose an integrated electronic maintenance framework (EMF) that utilizes information to monitor impairments and execute systematic maintenance for RIS elements. This framework aims to optimize service management in RIS-aided networks by extending the life cycle of the RIS and augmenting

[1]Note that this is fundamentally different from the transmitter hardware impairment caused by amplifier non-linearity, phase noise, and I/Q channel imbalance in the transmitter chain. For RIS hardware impairment, the degradation impact is modeled as affecting the signal after it has interacted with the RIS. In contrast, transmitter hardware impairment is applied directly to the transmitted signal, reflecting an impairment that occurs before the signal's interaction with the RIS or its propagation through the channel to the receiver.

the electronic reliability of the associated communication network. The EMF can reflect the current state of the RISs, including relevant historical data on the ECEs and the metasurfaces. The EMF can then be utilized to assess the RIS-aided physical network's current condition, predict its future behavior, refine control mechanisms, or optimize its operation in real-time. The EMF is applicable for an individual RIS element, a system composed of several RIS elements, or even an entire RIS-aided wireless network composed of both active and passive components for hybrid beamforming. Within this context, the primary distinctions of this work are summarized as follows:

- Electronic Maintenance Framework (EMF) for RIS: To overcome the constraints of inaccurate measurements by physical sensors in RIS-aided IIoT communication networks, we propose a novel framework called EMF that integrates stochastic modeling to monitor and evaluate the condition of RIS elements continuously. This framework is the first to address the ageing effects on RIS hardware systematically, determining optimal maintenance schedules to extend the operational life of RIS systems.
- Optimal Analytical Solutions within EMF: A significant contribution of our study is the derivation of optimal analytical solutions within the EMF to precisely time the maintenance activities. This approach helps in deciding whether maintenance should be performed immediately or can be postponed, optimizing for both the short-term functionality and long-term sustainability of the RIS system.
- Development of a Reliable Communication Framework *(RCF) under Imperfect Maintenance:* Recognizing the reality of imperfect maintenance, we introduce the RCF to assess and ensure reliable communication despite residual hardware impairments. This framework evaluates the error probability and signal-to-interference-plus-noise ratio (SINR) in RIS-aided systems, contributing to the robustness of communication under sub-optimal conditions.
- Comprehensive Analytical and Numerical Analysis: We provide an extensive analytical solution within the EMF to determine the optimal timing for RIS maintenance, balancing between immediate and deferred actions based on system conditions. Through simulations, we illustrate the reliability performance of RIS-aided communication systems under hardware impairments, validating the effectiveness of our proposed frameworks.

Apart from the above, our study underscores the environmental benefits of extending the RIS lifespan, contributing to the reduction of electronic waste and associated CO2 emissions. We also highlight the potential economic advantages of our frameworks in minimizing maintenance costs and preventing premature system failures in critical communication networks. By addressing hardware ageing and maintenance in RIS-aided systems, our work opens new avenues for future research, particularly in the optimization of maintenance strategies, digital twin and the exploration of advanced materials for RIS construction. The above contributions distinguish the proposed frameworks from traditional, static maintenance strategies, prevalent in industries pushing the boundaries of RIS longevity and cost-effectiveness. Importantly, the analysis in this work not only proposes delays in maintenance but also ensures network resilience against imperfect maintenance.

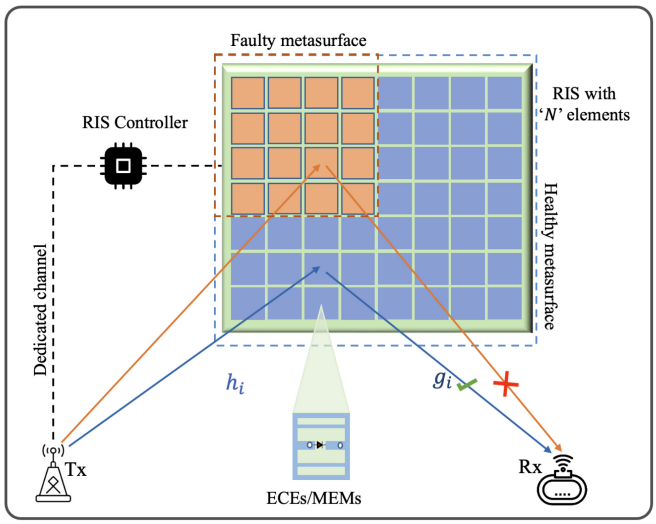

FIGURE 1. An illustration of a wireless environment augmented with a RIS with possible faulty elements, which may lead to disruption of communication due to the inaccurate reflection of the transmitted signal.

The rest of the paper is organized as follows. Section II provides the system model. In Section III, we present the EMF for RIS hardware. Section IV provides the electronic reliability analysis of the hardware-impaired RIS-aided system. Section V provides the RCF for RIS-aided communication under imperfect maintenance. Numerical results are presented in Section VI and finally, Section VII provides the concluding remarks.

Notations: $\mathrm{cov}(\mathbf{A})$, $\mathrm{var}(\mathbf{A})$, $\mathbb{E}[\cdot]$, $\mathbb{P}[\cdot]$ and $\mathbb{R}$ indicate the covariance of $\mathbf{A}$, the variance of $\mathbf{A}$, the expected value, probability, and real space, respectively.

II. SYSTEM MODEL

A communication network aided by a N-element RIS is considered as shown in Fig. 1, where the elements of the RIS have the sole functionality of actuators, which execute the commands from the transmitting node. The elements of the RIS are made up of metamaterials and are embedded with ECEs/MEMS that degrade with time. This degradation process results in hardware impairments of the system that are characterized by monotonically increasing sample paths and affect the system's reliability. We model the degradation of the RIS system by a stochastic process $\{X_t\}_{t\in T}$, where T is the index set and denotes the lifetime of the RIS system. We assume $T = [0, \infty)$ and that the state of the hardware impairment process $(X_t, t \geq 0)$, $X_0 = 0$ is captured

by the transmitting node at independent increments through dedicated control signals. Now, assuming a slowly varying and flat-fading channel model, the received signal reflected by a RIS from the transmitter to the receiver is given as

$$y = \sum_{i=1}^{N} h_i \exp(j\phi_i)\tilde{\kappa} g_i s + n, \tag{1}$$

where h_i and g_i are the communication channels from the transmitting node to RIS and from RIS to the receiver, respectively, ϕ_i is the adjustable phase induced by the ith reflecting meta-surface element of the RIS, s stands for the data symbol selected from an M-phase shift keying (MPSK) constellation with P being the average power corresponding to the transmitted symbol, $\tilde{\kappa}$ is the hardware impairment level observed by the transmitter at time $t_{\tilde{\kappa}}$ in the RIS,[2] and $n \sim \mathcal{CN}(0, N_0)$ is the additive white Gaussian noise (AWGN) at the receiver node. In the above, $0 < \tilde{\kappa} < \kappa$, where κ is a deterministic threshold of the impairment level. An outage in the network occurs when the hardware impairment level of the RIS system exceeds κ, whereby the level of impairment[3] overpowers the signal of interest for it to be properly decoded. Accordingly, the lifetime of the RIS system for proper signal reflection can be modeled by a normalized survival function[4] given as

$$\bar{S}(t, \kappa) = \Theta \bar{F}(t, \kappa). \tag{2}$$

Here, the survival function, denoted as $\bar{F}(t, \kappa)$, quantifies the likelihood that the RIS will maintain its operational integrity and performance over time, *i.e.,* without reaching a critical degradation threshold, κ, up to time t considering the stochastic nature of hardware degradation. This function is normalized by the parameter Θ to account for the varying initial conditions and operational environments of RIS systems, providing a standardized metric for comparing their longevity. Here,

$$\Theta = [\mathbf{1}\{\mathbb{P}(T > t)\}]\mathbf{1}\{\text{RIS is active}\}, \tag{3}$$

where the indicator function $\mathbf{1}\{A\}$ is equal to one if the event A occurs and zero otherwise. Moreover, $\bar{F}(t, \kappa)$ in (2) can be described as

$$\mathbb{P}(T > t) \equiv \bar{F}(t, \kappa) = \mathbb{P}(X_t \leq \kappa). \tag{4}$$

If t is fixed, then $\bar{F}(t, \kappa)$ becomes the cumulative distribution function (CDF) of the random variable X_t. In contrast, if κ is fixed, it becomes the survival function of the random variable T. Accordingly, the CDF $F(t, \kappa) = 1 - \bar{F}(t, \kappa) = \mathbb{P}(X_t > \kappa)$.

[2]We assume that the impairment level is uniform across all N reflecting elements of the RIS, i.e., $\tilde{\kappa}_i = \tilde{\kappa}, \forall i = \{1, 2, \ldots, N\}$, where $\tilde{\kappa}_i$ is the impairment level of the ith RIS element.

[3]Under this scenario, any of the N elements of the RIS fail to reflect the signal of the transmitter in the desired direction.

[4]The survival function of the RIS system is the complementary cumulative distribution function (CCDF) of the lifetime of the RIS system T.

III. ELECTRONIC MAINTENANCE FRAMEWORK FOR RIS HARDWARE

In the EMF layer, the digital replication of the physical entities, such as the non-residual hardware impairment level of the RIS and the degradation process, provides the dynamics of the model. The EMF maps the statistical information of the state of the RIS elements to augment the current RIS hardware condition into virtual surface elements, thus, identifying the impairments in the RIS elements and accommodating them with appropriate statistical modeling. The EMF's design and functionality is illustrated below:

1) FRAMEWORK OVERVIEW

The EMF is conceptualized as a digital replication of hardware and software components that continuously assess the operational health of RIS elements and predict their degradation trajectory. It leverages statistical models to inform maintenance decisions, aiming to address degradation before it preemptively impacts system performance. We map the statistical information of the state of the RIS elements to augment the current RIS hardware condition into virtual surface elements, thus identifying the impairments in the RIS elements and accommodating them with appropriate statistical modeling.

2) CORE COMPONENTS OF THE EMF

- Degradation Prediction Module: Utilizes stochastic models, including the Poisson process, to predict the rate and occurrence of hardware degradation events based on historical data and operational parameters.
- Maintenance Decision Logic: Analyzes predictions and simulated data (representing the data generated by actual sensors embedded in an operational RIS) to determine optimal maintenance schedules, balancing the need for preventive maintenance against the RIS's operational demands and lifecycle management objectives.
- Maintenance Execution Interface: Facilitates the implementation of maintenance actions, from software adjustments to physical repairs or component replacements, as the Maintenance Decision Logic dictates.

3) INTEGRATION WITHIN THE RIS SYSTEM

The EMF can be integrated into the RIS system through both hardware interfaces (for monitoring and maintenance execution) and software APIs (for data exchange and control logic). This integration will ensure that the EMF can operate seamlessly with the RIS to enhance its reliability and extend its lifespan.

To replicate the EMF for the observed impairment $\tilde{\kappa}$, if X_t is homogeneous with a constant parameter λ, then the remaining lifetime of the RIS system T_{RL} does not depend on $t_{\tilde{\kappa}}$ and is characterized by the normalized survival function $\bar{S}(t, \kappa - \tilde{\kappa}) = \Theta \bar{F}(t, \kappa - \tilde{\kappa})$, where

$$\bar{F}(t, \kappa - \tilde{\kappa}) = \mathbb{P}(X_t \leq \kappa - \tilde{\kappa}). \tag{5}$$

However, if X_t is non-homogeneous with a variable parameter $\lambda(t)$, the remaining lifetime of the RIS system depends on $t_{\tilde{\kappa}}$. From (4), for fixed $\tilde{\kappa}$, the CDF of $t_{\tilde{\kappa}}$ is given as $F(t,\tilde{\kappa}) = 1 - \bar{F}(t,\tilde{\kappa})$. Accordingly, the remaining lifetime T_{RL} can be characterized by the normalized survival function $\bar{S}(t,\kappa,\tilde{\kappa}) = \Theta\bar{F}(t,\kappa,\tilde{\kappa})$, where

$$\mathbb{P}(T_{RL} > t) \equiv \bar{F}(t,\kappa,\tilde{\kappa}) = \mathbb{P}\big(X_{t_{\tilde{\kappa}}+t} - X_{t_{\tilde{\kappa}}} \leq \kappa - \tilde{\kappa}\big). \quad (6)$$

We assume that the stochastic degradation of the RIS is modeled in the EMF as a Poisson process Φ with rate λ. Furthermore, let the hardware impairment affect the N RIS elements in an independent, identically distributed (i.i.d.) and exponentially distributed manner. Then the survival function of the waiting time, until the N-th element of the RIS fails due to hardware impairment, can be represented for a homogeneous Poisson process (HPP) in the EMF as

$$\begin{aligned}\bar{F}(t,N) &= \mathbb{P}\big(X_{t_{\tilde{\kappa}}+t} - X_{t_{\tilde{\kappa}}} < N\big) \\ &= \exp\{-\lambda * t\} \sum_{i=0}^{N-1} \frac{(\lambda * t)}{t!};\ \forall \kappa > 0. \end{aligned} \quad (7)$$

Here, the failure rate λ can be expressed as

$$\lambda(t,N) = \frac{\lambda^N t^{N-1}}{(N-1)! \sum_{k=0}^{N-1} \frac{(\lambda * t)^k}{k!}}, \quad (8)$$

which is a monotonically increasing function. The communication network goes into outage when the Nth RIS element fails. Thus, the remaining lifetime on observing $n < N$ elements (events) is given by

$$F(t,N-n) = 1 - \exp\{-\lambda * t\} \sum_{j=0}^{(N-n)-1} \frac{(\lambda * t)^j}{j!}, \quad (9)$$

which clearly indicates that for each $t > 0$ the corresponding failure rate is increasing in n.

In the event that the degradation of RIS do not strictly follow a Poisson process, alternative stochastic models could potentially describe the degradation behavior. This includes models like the non-homogeneous Poisson Process (NHPP), which allows for the rate of degradation events to vary over time, and the Gamma process, known for its flexibility in modeling a wide range of failure rate behaviors. For example, for a non-homogeneous Poisson process (NHPP), using Eq. (6) the corresponding remaining lifetime at $T_{\tilde{\kappa}}$ is given as

$$\mathbb{P}\big(X_{t_{\tilde{\kappa}}+t} - X_{t_{\tilde{\kappa}}} < N\big) = \exp\{-\Gamma(t_{\tilde{\kappa}},t)\} \sum_{i=0}^{N-1} \frac{(\Gamma(t_{\tilde{\kappa}},t))^i}{i!}, \quad (10)$$

where $\Gamma(t_{\tilde{\kappa}},t) = \int_{t_{\tilde{\kappa}}}^{t_{\tilde{\kappa}}+t} \lambda(y)dy$ and $\lambda(t)$ is the rate of NHPP. Accordingly, for the observed $n < N$ elements (events), the corresponding remaining lifetime can be expressed as

$$\begin{aligned} &F(t,T_{\tilde{\kappa}},N-n) \\ &\quad = 1 - \exp\{-\Gamma(t_{\tilde{\kappa}},t)\} \sum_{m=0}^{(N-n)-1} \frac{(\Gamma(t_{\tilde{\kappa}},t))^m}{m!}. \end{aligned} \quad (11)$$

With the above EMF, our goal is to improve the reliability of the RIS-aided network by extending the lifetime of the RIS system. Accordingly, in the following section, we formulate the mathematical framework for performing systematic maintenance under two scenarios: a) at a predefined time and state of the RIS and b) based on specific discrete information captured by the transmitter through dedicated control signals. For tractability, we assume that $\mathbb{P}(T > t)$ and the RIS is active until failure. Hence, hereinafter, the normalized survival function $\bar{S}(t,\kappa)$ is represented by $\bar{F}(t,\kappa)$. At this point we would like to note that the mathematical expressions required for the non-homogeneous case tend to become quite complex. Nevertheless, by concentrating on the homogeneous scenario, we can still fully analyze the RIS life cycle without the added complexity introduced by the non-homogeneous processes. Hence, hereinafter we provide the results for the homogeneous process only, while the generalization for the non-homogeneous case is left for future work.

Remark 1 (Choice of RIS Degradation Model): Our choice of the RIS degradation model is based on observed phenomena in similar advanced electronic systems exposed to environmental stresses over time [18], [19], [27]. The model accounts for the cumulative effect of factors such as temperature fluctuations, mechanical stress, and electromagnetic exposure, which align with documented cases of hardware degradation in literature. Since this degradation process is characterized by monotonically increasing sample paths, decreasing the lifespan of the RIS, and affecting the reliability of the system, we model the degradation process by a stochastic process. Next, the hardware impairment factor model arising from the RIS degradation incorporates both deterministic and stochastic elements to realistically simulate the varying nature of hardware degradation. The model's formulation is grounded in the principle of wear and tear experienced by electronic components over time, a well-documented phenomenon in electronic engineering research. Accordingly, in this work, we model the degradation process as a Poisson process due to the fact that it can express the corresponding jump process by representing the hardware impairment factors *i.e.,* κ and $\tilde{\kappa}$ as integers. This assumption is reasonable as degradation of the metamaterial of the RIS system including the electronic semiconductors typically follows a monotonic pattern, and the errors are classified in literature [28], [29] as i) independent, ii) clustered, iii) aligned, or state-specific. A general methodology for the analysis of errors in RISs would simply be to evaluate the RISs' metasurface in the presence of an increasing number of errors. To set the position of the faulty RIS elements according to spatial distribution, the Poisson process is widely used in metasurface literature [30], [31].

Remark 2 (RIS Impairment Estimation): The estimation of channel state information including the RIS impairment level in the network within the EMF follows a similar strategy to that of traditional systems. This can be performed via the exchange of the training sequences and feedback

between the transmitter and the receiver reflected through the RIS at regular intervals either in time division duplex (TDD) or frequency division duplex (FDD) mode. The received pilot sequences can be used to estimate the level of degradation in the RIS elements. Alternatively, an estimate of the hardware impairment in the RIS can be obtained utilizing the RIS controller, which oversees the operation and configuration of the RIS elements, and is directly connected to the transmitter. This assessment can be accomplished by leveraging a sensor network deployed within the RIS, capable of detecting and communicating the impairment level between the RIS and the transmitter via the RIS controller. Both methods enable a continuous feedback loop where the condition of the RIS hardware, including any impairments or degradation, is relayed back to the transmitter in real-time. This feedback mechanism is fundamental to the operation of RIS-aided communication systems [32], [33], [34], allowing for dynamic adjustments to the RIS configuration to optimize communication performance in light of any detected hardware impairments.

IV. ELECTRONIC RELIABILITY ANALYSIS

A. BLIND RATIONALIZATION WITHOUT PRIOR INFORMATION

This scenario deals with the case when we want to prolong the life of a RIS system with no prior history of impairments. We can extend the time to failure by performing optimal systematic maintenance at some time δ.

Implementing systematic maintenance too early will have negligible effects on the RIS system as the elements might not have degraded enough. On the other hand, if the time δ is too large then there is a high likelihood that a failure will occur before the specified maintenance time. Now, to calculate the optimal maintenance time δ^*, we first consider the case with one systematic maintenance. A generalized case of multiple maintenances will be presented later.

Let us consider the EMF of a RIS system with a life cycle denoted by (4). Let $m_1(\delta, \kappa)$ denote the mean time to failure for the system and assume that one perfect systematic maintenance[5] is performed at $t = \delta$. Then the corresponding mean time to failure for the observed degradation at $t_{\tilde{\kappa}} \in [0, \delta)$, in accordance with its conditional probability is given by

$$\begin{aligned} m_1(\delta, \kappa) &= F(\delta, \kappa)\mu(\delta, \kappa) + \bar{F}(\delta, \kappa)(\delta + m(\kappa)) \\ &= \int_0^{\delta} \bar{F}(t_{\tilde{\kappa}}, \kappa) dt_{\tilde{\kappa}} + \bar{F}(\delta, \kappa) m(\kappa). \end{aligned} \tag{12}$$

Here,

$$\mu(\delta, \kappa) = \frac{\int_0^{\delta} \big(\bar{F}(t_{\tilde{\kappa}}, \kappa) - \bar{F}(\delta, \kappa)\big) d\kappa}{F(\delta, \kappa)} \tag{13}$$

is the conditional expected lifetime, given that the failure occurred in $[0, \delta)$, and

$$m(\kappa) = \int_0^{\infty} \bar{F}(t_{\tilde{\kappa}}, \kappa) d\kappa \tag{14}$$

is the mean time to failure of the RIS system before the systematic maintenance.

Proposition 1: Assume that the failure rate of the RIS system in (8) is strictly increasing in t and $\lambda(t, N) \to \lambda$, $t \to \infty$. If one systematic maintenance is applied to the RIS system at time δ, then an optimal solution for the mean time to failure exists, *i.e.,*

$$m_1\big(\delta^*, \kappa\big) = \max_{\delta \geq 0} m_1(\delta, \kappa), \tag{15}$$

where

$$\delta^* = \lambda^{-1}(1/m(\kappa), \kappa) \tag{16}$$

is a unique solution. Here, $\lambda^{-1}(\cdot, \cdot)$ is the inverse function of the failure rate $\lambda(\cdot, \cdot)$.

Proof: The proof is given in Appendix A. ■

A generalized expression for the mean time to failure of the RIS system, when multiple systematic maintenances are considered, is given in the below proposition.

Proposition 2: If multiple systematic maintenances are applied to the RIS system at times $\delta_1, \delta_1 + \delta_2, \ldots, \delta_1 + \delta_2 + \cdots + \delta_n$ with inter-PM times δ_i $i = 1, 2, \ldots, n$, then an optimal solution for the mean time to failure exists, *i.e.,*

$$m_n\big(\delta_1^*, \delta_2^*, \ldots, \delta_n^*; \kappa\big) = \max_{\delta \geq 0; i=1,2,\ldots,n} m_n(\delta_1, \delta_2, \ldots, \delta_n; \kappa). \tag{17}$$

Proof: The proof is given in Appendix B. ■

B. INFORMATION-FUSED EMF

This scenario deals with the case when the operation of the RIS is fully monitored by the transmitter through dedicated control signals.[6] The information about the impairment level at the EMF is deterministic and systematic maintenance is applied just before reaching the threshold κ. Let us consider the optimal δ^* as obtained in Proposition 1 and assume that the transmitter calculates the impairment value of the RIS system at time δ^*. Denoting this impairment value to be $\tilde{\kappa}$, we can declare that the RIS can function till an impairment level equivalent to $\kappa - \tilde{\kappa}$ is reached. Now, the EMF uses this information to delay systematic maintenance, thus increasing the remaining lifetime of the RIS system. Accordingly, the maintenance is performed at $\delta^* + \delta_1$ instead of performing it at δ^*. This will maximize the mean remaining lifetime after $t = \delta^*$. Accordingly, (12) can be rewritten to give the information-based mean time to failure of the RIS system as

$$m_1(\delta_1, \kappa, \tilde{\kappa}) = \int_0^{\delta_1} \bar{F}_{\tilde{\kappa}}(t_{\tilde{\kappa}}) dt_{\tilde{\kappa}} + \bar{F}_{\tilde{\kappa}}(\delta_1) m(\kappa). \tag{18}$$

[5]A perfect systematic maintenance means that after maintenance, the system behaves like new. The impact of imperfect maintenance will be considered in Section IV.

[6]In practical systems, continuous monitoring may not be feasible. So, discrete monitoring can be implemented.

Now, let us consider $\lambda_{\tilde{\kappa}}(t)$ to be the failure rate corresponding to the remaining lifetime $F_{\tilde{\kappa}}(t)$ of the RIS system with observed degradation $\tilde{\kappa}$. As the remaining threshold, $\kappa - \tilde{\kappa}$ decreases, the failure rate increases for $t > 0$. Hence,

$$\lambda_{\tilde{\kappa}_1}(t) < \lambda_{\tilde{\kappa}_2}(t); \tilde{\kappa}_1 < \tilde{\kappa}_2 < \kappa, \forall t > 0. \tag{19}$$

Now, from (18) we have the following

$$m_1(0, \kappa, \tilde{\kappa}) = m(\kappa), \tag{20}$$

$$m_1(\infty, \kappa, \tilde{\kappa}) = \int_0^\infty \bar{F}_{\tilde{\kappa}}(t_{\tilde{\kappa}}) dt_{\tilde{\kappa}} < m(\kappa). \tag{21}$$

Our aim is to find the optimal solution for the mean time to failure. Similar to the blind rationalization case, the optimal value can be calculated by first taking the partial derivative of (18) as

$$m_1'(\delta_1, \kappa, \tilde{\kappa}) = \bar{F}_{\tilde{\kappa}}(\delta_1)(1 - \lambda_{\tilde{\kappa}}(\delta_1) m(\kappa)). \tag{22}$$

Next, as $\lambda_{\tilde{\kappa}}(\delta_1)$ is increasing in δ_1, we can infer from (21) and (22) that if $\lambda_{\tilde{\kappa}}(0)m(\kappa) \geq 1$, then $\lambda_{\tilde{\kappa}}(\delta_1)m(\kappa) \geq 1$, $\delta_1 > 0$. Hence, $m_1(\delta_1, \kappa, \tilde{\kappa})$ is decreasing in δ_1, thus suggesting that the systematic maintenance of the RIS system must be performed immediately at $t = \delta^*$.

Proposition 3: If $\lambda_{\tilde{\kappa}}(0)m(\kappa) < 1$ holds then for the observed impairment $\tilde{\kappa}$, there exists an optimal ${\delta_1}^* > 0$ that gives the optimal remaining mean time to failure of the RIS system as

$$m_1\left(\delta^*, \delta_1^*, \kappa, \tilde{\kappa}\right) = m_1\left(\delta^*, \kappa\right) + \bar{F}\left(\delta^*, \kappa\right)\left(m_1\left(\delta_1^*, \kappa, \tilde{\kappa}\right) - m(\kappa)\right). \tag{23}$$

Proof: First, we show that the inequality $\lambda_{\tilde{\kappa}}(0)m(\kappa) < 1$ holds that will guarantee that the function $m_1(\delta_1, \kappa, \tilde{\kappa})$ is increasing in $[0, \varepsilon)$ for some $\varepsilon > 0$, and hence the internal maximum exists.

Leveraging the analysis in Appendix A, we can show that

$$\lambda_{\tilde{\kappa}}(\delta_1) m(\delta_1, \kappa, \tilde{\kappa}) = m'(\delta_1, \kappa, \tilde{\kappa}) + 1, \tag{24}$$

where,

$$m(\delta_1, \kappa, \tilde{\kappa}) \equiv \int_0^\infty \exp\left\{-\int_0^t \lambda_{\tilde{\kappa}}(\delta_1 + t_{\tilde{\kappa}}) dt_{\tilde{\kappa}}\right\} dt.$$

As $\lambda_{\tilde{\kappa}}(\delta_1)$ is strictly increasing in δ_1, the corresponding mean remaining lifetime $m(\delta_1, \kappa, \tilde{\kappa})$ is decreasing. Thus, $m'(\delta_1, \kappa, \tilde{\kappa}) < 0$ results in $\lambda_{\tilde{\kappa}}(\delta_1)m(\delta_1, \kappa, \tilde{\kappa}) < 1, \forall \delta_1 \geq 0, \forall 0 \leq \tilde{\kappa} < \kappa$. Therefore, the inequality can be satisfied under a certain condition. Also, for $(\tilde{\kappa} = 0)$, we have

$$\lambda_0\left(\delta^*\right) m(\kappa) = 1 \Rightarrow \lambda_0(0) m(\kappa) < 1.$$

Thus, $\tilde{\kappa}$ can increase from 0 to some $\hat{\kappa}$ and the inequality will still be valid (see equation (19) (when $\lambda_{\tilde{\kappa}_1}(0) = \lambda_{\tilde{\kappa}_2}(0) = 0$ for all $\tilde{\kappa}_1 < \tilde{\kappa}_2 < \kappa$, the inequality always, obviously, holds). Thus, when $0 \leq \tilde{\kappa} < \hat{\kappa}$, inequality holds and, therefore, the optimal ${\delta_1}^*$ exists.

From the above reasoning, there exists an optimal ${\delta_1}^* > 0$ when $m_1(\delta_1, \kappa, \tilde{\kappa})$ achieves its maximum value, *i.e.,* $m_1(\delta_1^*, \kappa, \tilde{\kappa})$. Accordingly, the maximum mean time to failure in (15) can be increased to the one given in (23). ■

V. RELIABLE COMMUNICATION FRAMEWORK UNDER IMPERFECT MAINTENANCE

In order to characterize the reliability of the RIS-aided communication system, in this section, we develop a RCF and measure the performance of the considered system in terms of BEP and BER. Here, we take into consideration the miss-measurement and incorrect estimation and assume imperfect maintenance of the RIS elements, thereby producing residual impairment. This residual impairment is modeled as an additive stochastic parameter that is independent of the communication channel. In particular, an additive white Gaussian "RIS noise" with variance η times the energy of the transmit signal is applied to the system through the source-RIS-destination communication channel. Accordingly, the parameter $\tilde{\kappa}$ in (1) can now be modeled within the RCF to reflect the residual impairment as

$$\tilde{\kappa} \sim \mathcal{CN}(0, \eta P). \tag{25}$$

The aforementioned error model is suitable for cases where the error is mainly due to hardware estimation inaccuracies. The parameter[7] η, hereinafter will be referred to as the RIS-distortion and can be assumed to be known a priori and $\eta < 0$dB.

Now, after writing the channels in the RIS-aided system from Section II in terms of amplitudes and phases, *i.e.*, $h_i = \alpha_i e^{-j\theta_i}$, $g_i = \beta_i e^{-j\psi_i}$, where α and β are the amplitudes, and θ and ψ are the phases of the channels h_i and g_i respectively. The instantaneous SINR can be given from (1) as

$$\gamma = \frac{\left|\sum_{i=1}^N \alpha_i \beta_i e^{(\phi_i - \theta_i - \psi_i)}\right|^2 P}{\left[\left|\sum_{i=1}^N \alpha_i \beta_i e^{(\phi_i - \theta_i - \psi_i)}\right|^2\right] \eta P + N_0}. \tag{26}$$

Lemma 1: Let $\zeta_i \in \mathbb{R}$ and $0 \leq \nu_i \leq 2\pi$, $\forall i \in \{1, \ldots, N\}$. Then, $|\sum_{i=1}^N \zeta_i e^{j\nu_i}|^2$ is maximized by setting $\nu_i = \nu$, $\forall i$.

Proof: This can be proved by first expanding $|\sum_{i=1}^N \zeta_i e^{j\nu_i}|^2$ as

$$\left|\sum_{i=1}^N \zeta_i e^{j\nu_i}\right|^2 = \sum_{i=1}^N \zeta_i^2 + 2\sum_{i=1}^N \sum_{k=i+1}^N \zeta_i \zeta_k \cos(\nu_i - \nu_k) \tag{27}$$

and then setting $\nu_i = \nu$, $\forall i$. ■

From (26), it is easy to observe that, the SINR is maximized when the channel phases are removed. This can be achieved by intelligently adjusting the phase shifts[8] of the RIS such that $\phi_i = \theta_i + \psi_i$, $\forall\ i = 1, 2, \ldots, N$, as shown in Lemma 1. Accordingly, the maximized instantaneous received SINR can be expressed

$$\gamma_{\max} = \frac{\left(\sum_{i=1}^N \alpha_i \beta_i\right)^2 P}{\left(\sum_{i=1}^N \alpha_i \beta_i\right)^2 \eta P + N_0} = \frac{AP}{A\eta P + N_0}. \tag{28}$$

[7]This model has been validated for measuring the non-ideality of RF chains through hardware measurements in [35] and [36].

[8]This work assumes perfect phase shift adjustments. Deviations from perfect phase shift adjustment can be incorporated into the model as additional factors or uncertainties.

Here, α_i and β_i can be considered independent Rayleigh distributed random variables. Now, following the properties of Rayleigh distribution, $\mathbb{E}[A] = \mathbb{E}[\alpha_i\beta_i] = \frac{\pi}{4}$ and $\text{Var}[A] = \text{Var}[\alpha_i\beta_i] = 1 - \frac{\pi^2}{16}$.

Lemma 2: Consider two random variables R and S, where S either has no mass at 0 (discrete) or has support [0;1). Let $G = g(R; S) = R/S$. Further, let $\mathbb{E}[R] = \mu_R$ and $\mathbb{E}[S] = \mu_S$. The mean and variance of G can respectively, be given as

$$\mathbb{E}\left[\frac{R}{S}\right] \approx \frac{\mu_R}{\mu_S} - \frac{\text{cov(R,S)}}{(\mu_S)^2} + \frac{\text{Var}(S)\mu_R}{(\mu_S)^3},$$
$$\text{Var}\left(\frac{R}{S}\right) = \left(\frac{\mu_R}{\mu_S}\right)^2\left[\frac{\sigma_R^2}{(\mu_R)^2} - \frac{2\text{cov(R, S)}}{\mu_R\mu_S} + \frac{\sigma_S^2}{(\mu_S)^2}\right].$$

Proposition 4: When the number of elements in the RIS is asymptotically large, i.e., $N \gg 1$, *i.e.*, the mean (μ) and variance (σ) of the maximized received SINR for the considered RIS-aided system are respectively given as

$$\mathbb{E}[\gamma_{\max}] = \frac{PN\pi}{4\left[\frac{N\pi}{4}\eta P + N_0\right]^3} \times \left[\left[\frac{N\pi}{4}\eta P + N_0\right]^2 + N\left(1 - \frac{\pi^2}{16}\right)(\eta P)^2\right] \quad (29)$$

and

$$\text{Var}(\gamma_{\max}) = \left[\frac{N^2\frac{\pi^2}{16}}{\left(\frac{N\pi}{4}\eta P + N_0\right)^2}\left\{\frac{N\left(1 - \frac{\pi^2}{16}\right)}{N^2\frac{\pi^2}{16}} + \frac{\left(N\left(1 - \frac{\pi^2}{16}\right)\right)(\eta P)^2}{\left(\frac{N\pi}{4}\eta P + N_0\right)^2}\right\}\right]P^2. \quad (30)$$

Proof: The proof is given in Appendix C. ■

Proposition 5: For $N \gg 1$, $(\gamma_{\max} + \mu)^2$ exhibits a non-central chi-squared distribution with one degree of freedom, and the corresponding moment-generating function (MGF) of γ_{max} can be expressed as (31), shown at the bottom of the page.

Proof: The proof is given in Appendix D. ■

Lemma 3 [37]: Let φ be the SINR at the receiver of a wireless communication system and p_φ be its PDF. Then, the average symbol error probability (SEP) at the receiver is given by

$$\text{SEP} = \int_0^\infty Q\left(a\sqrt{\varphi}\right)p_\varphi(\varphi)d\varphi. \quad (32)$$

Here, a is a constant that depends on the specific modulation/detection combination, $Q(k)$ is the one-dimensional Gaussian Q-function corresponding to the normalized Gaussian random variable K, given as

$$Q(k) = \frac{1}{\pi}\int_0^{\pi/2}\exp\left(-\frac{k^2}{2\sin^2 w}\right)dw. \quad (33)$$

Using Lemma 3, we obtain the average BEP performance of the RIS-aided system for M-PSK signaling as

$$\begin{aligned}\text{BEP} &\overset{(a)}{=} \frac{1}{\log_2^M}\int_0^\infty\frac{1}{\pi}\int_0^{\frac{(M-1)\pi}{M}}\exp\left(-\frac{a^2\varphi}{2\sin^2 w}\right)dw p_\varphi(\varphi)d\varphi \\ &= \frac{1}{\pi\log_2^M}\int_0^{\frac{(M-1)\pi}{M}}\left[\int_0^\infty\exp\left(-\frac{\text{a}^2\varphi}{2\sin^2\text{w}}\right)\text{p}_\varphi(\varphi)\text{d}\varphi\right]dw \\ &\overset{(b)}{=} \frac{1}{\pi\log_2^M}\int_0^{(M-1)\pi/M}M_{\gamma_{\max}}\left(\frac{-\sin^2(\pi/M)}{\sin^2 w}\right)dw. \end{aligned} \quad (34)$$

Here, (a) is obtained using the relation $\text{BEP} = \text{SEP}/\log_2^{\text{M}}$ and (b) is obtained using (31) specifically for $a^2 = 2\sin^2(\pi/M)$. Now, the number of bit errors relative to the total number of transmitted bits b per symbol can be given using the metric BER, which can be calculated as $\text{BER} = \text{BEP}/b$.

VI. NUMERICAL RESULTS

In this section, we validate the analytical results developed for EMF and RCF through numerical computation. Given the scarcity of comparable studies, our simulation approach leverages theoretical models and assumptions grounded in the general principles of electronic component degradation and maintenance. These models are informed by established practices in related fields, adapted to the unique context of RIS technology. Accordingly, we rely on simulated data that models the degradation process of RIS elements over time, using parameters taken from standard literature on electronic component degradation and RIS characteristics. This approach allows us to project the potential impact of the EMF on RIS longevity and reliability, within the constraints of currently available knowledge. For the sake of analysis, we consider one possible systematic maintenance. The impairment threshold κ is taken as a normalized deterministic value equal to observing the N-th event of

$$M_{\gamma_{\max}}(t) = \left(1 - 2\left(\left[\frac{N^2\frac{\pi^2}{16}}{\left(\frac{N\pi}{4}\eta P + N_0\right)^2}\left\{\frac{N\left(1 - \frac{\pi^2}{16}\right)}{N^2\frac{\pi^2}{16}} + \frac{N\left(1 - \frac{\pi^2}{16}\right)(\eta P)^2}{\left(\frac{N\pi}{4}\eta P + N_0\right)^2}\right\}\right](P)^2\right)t\right)^{-\frac{1}{2}} \times \exp\left[\frac{4\left(\left[\frac{N\frac{\pi}{4}}{\frac{N\pi}{4}\eta P + N_0} + \frac{N\left(1-\frac{\pi^2}{16}\right)(\eta P)^2\frac{N\pi}{4}}{\left[N\frac{\pi}{4}\eta P + N_0\right]^3}\right]P\right)^2 t}{1 - 2\left(\left[\frac{N^2\frac{\pi^2}{16}}{\left(\frac{N\pi}{4}\eta P + N_0\right)^2}\left\{\frac{N\left(1-\frac{\pi^2}{16}\right)}{N^2\frac{\pi^2}{16}} + \frac{\left(N\left(1-\frac{\pi^2}{16}\right)\right)(\eta P)^2}{\left(\frac{N\pi}{4}\eta P + N_0\right)^2}\right\}\right](P)^2\right)t}\right]. \quad (31)$$

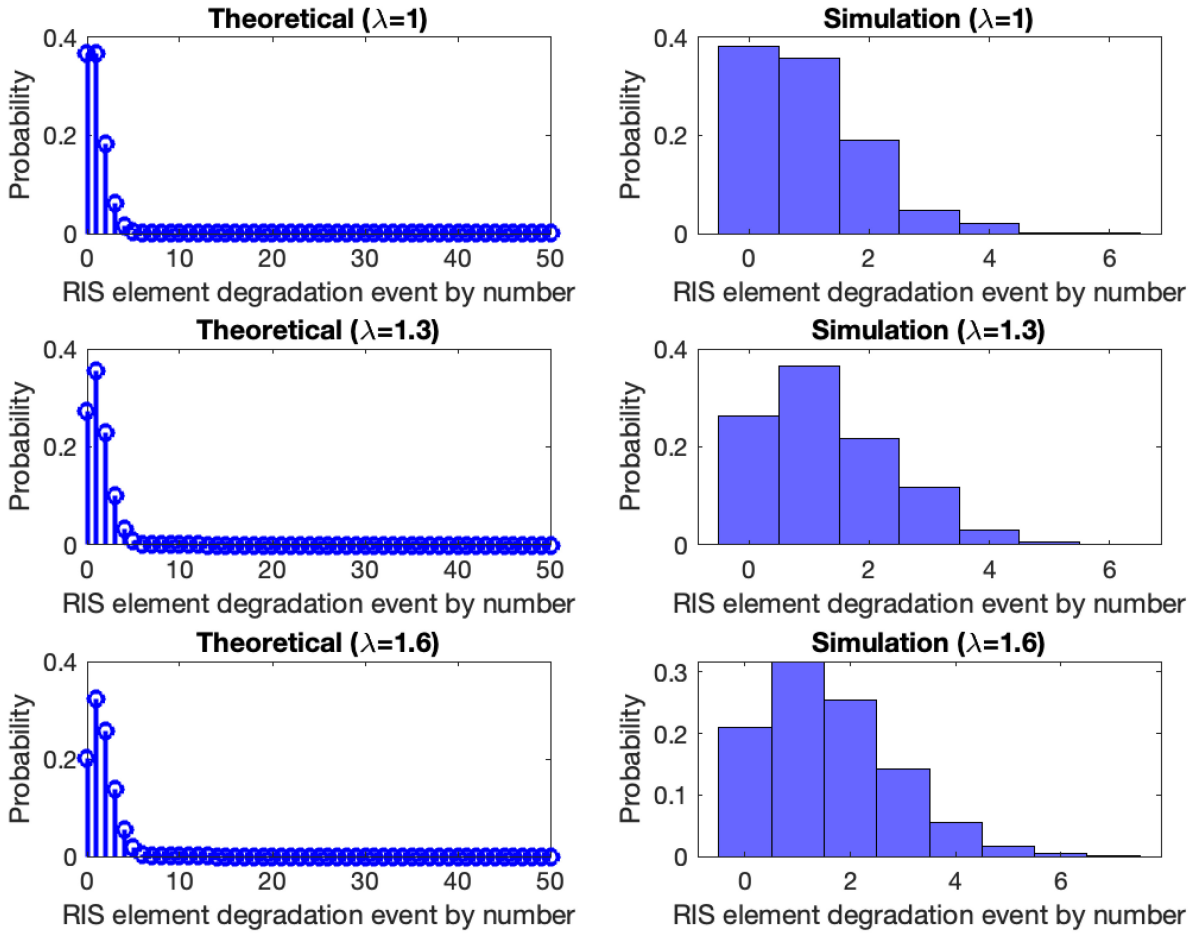

FIGURE 2. Distribution of RIS hardware degradation (theoretical vs simulation) for various λ.

failure. Unless otherwise stated we consider $N = 32$, and the failure rate λ is varied as $\lambda = \{1.0, 1.3, 1.6\}$ throughout the analysis.[9] Uncorrelated Rayleigh fading channels are considered to measure the BEP and BER of the RIS-aided network.

We begin by comparing the theoretical and simulated distribution of the survival function of the RIS hardware in Fig. 2. It can be seen from the figure that the histogram for 1000 simulations approximates the theoretical mass function for $N = 50$ for various values of the parameter λ. After validating the theoretical distribution with simulation, the distribution in the corresponding figures is generated in a similar fashion with equivalent parameters.

Now, we show the expected lifetime of the RIS system for the blind rationalization case in Fig. 3. The curves are plotted using (12) with respect to the time[10] at which systematic maintenance is performed for different values of λ. This figure shows the optimal maintenance time. The maximum values 53.69, 41.31 and 33.56 are achieved at $\delta^* = 24, 18.5$ and 15, respectively. Furthermore, the expected life cycle of the RIS system without maintenance is given as $m(32) = 32/\lambda$, which is illustrated by the straight curves. It is implicit from the figure that the proposed EMF framework can

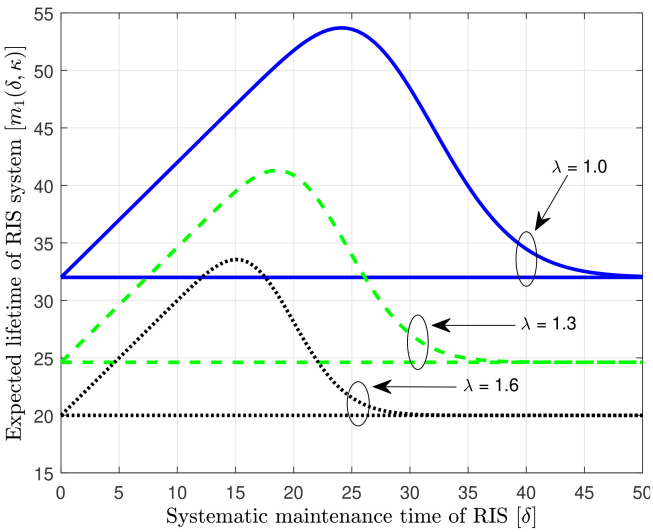

FIGURE 3. Expected mean lifetime of the RIS system vs systematic maintenance time for blind rationalization.

[9]The simulation parameters are based on widely used literature on reliability analysis [27], [38].

[10]The time on the *y*-axis of Fig. 3–Fig. 6 is a subjective understanding of time that is not constrained by specific numerical values, units, or divisions.

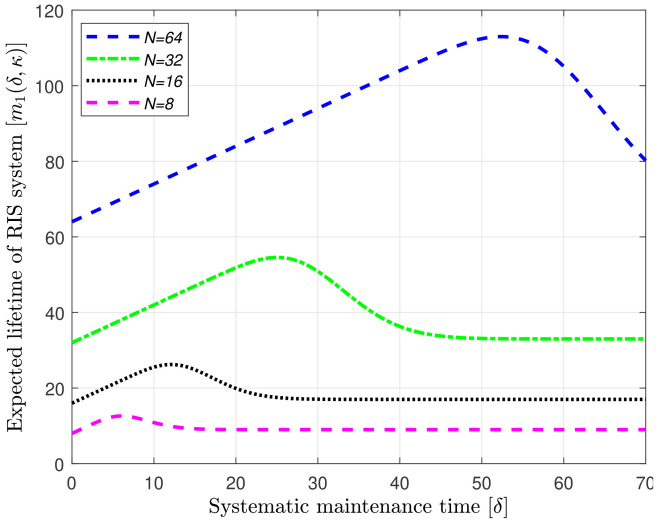

FIGURE 4. Expected mean lifetime of the RIS-system versus systematic maintenance time for a varying number of RIS elements, for $\lambda = 1.0$.

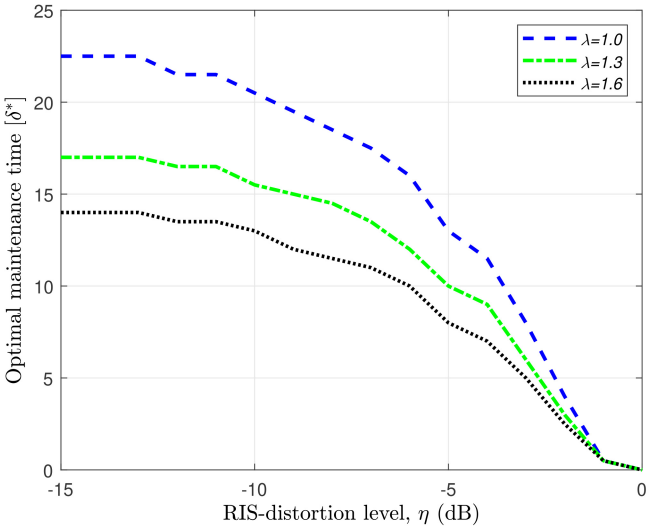

FIGURE 5. Optimal systematic maintenance time versus observed distortion by the transmitter.

optimally initiate repairs to mitigate the hardware impairment in the RIS system that can extend its lifetime. Furthermore, the impact of the impairment can also be reduced and the lifetime of the RIS can be increased by increasing the number of RIS elements, which is illustrated in Fig. 4 for $\lambda = 1.0$. The observed trend of a longer expected lifetime with a larger number of reflecting elements (N) in this figure can be attributed to the distributed nature of impairments across the RIS. As N increases, the impact of degradation in any single element becomes relatively diluted across the entire RIS, allowing for a more uniform distribution of the signal reflection and maintenance of operational efficiency even as individual elements begin to degrade. This distribution effect ensures that the RIS can sustain its functional performance over a longer period before the cumulative impairments significantly compromise the overall system performance.

Next, in Fig. 5 we consider the information-fused EMF scenario. Here, we show the optimal maintenance time with respect to the observed impairment level $\tilde{\kappa}$ for various λ using (23). This figure basically illustrates the level by which systematic maintenance can be delayed if a certain level of impairment is observed by the transmitter during dedicated inspection of the RIS system at the blind optimal δ^*. For example, it can be seen from the figure that for $\lambda = 1.0$, when the RIS distortion level is $\eta = -6$dB (*i.e.,* the observed degradation $\tilde{\kappa} = 9.44$dB for $P = 45$dBm), the postponement is ≈ 16, which is quite significant considering that the blind optimal maintenance time for this particular case is 24 as was observed in Fig. 3.

In Fig. 6, we show the achievable gain with respect to the longevity of the RIS system when one systematic maintenance is performed as soon as the transmitter observes the impairment $\tilde{\kappa}$ at the optimal time δ^*. For example, it can be seen from the figure that when $\lambda = 1.0$, the minimal life expectancy of the RIS system $m_1(\delta^*, \delta_1^*, \kappa, \tilde{\kappa}) = m_1(24, 0, 32, 32) = 53.69$, which is equivalent to the blind rationalization case. It can be seen that the life expectancy monotonically increases when the observed impairment level decreases and reaches a value of $m_1(24, 24, 32, 0) = 73.93$. Therefore, we can conclude that the proposed information-fused EMF can significantly extend the expected life of a RIS system when compared to the scenario with blind rationalization, where when the systematic maintenance is carried out at the optimal time δ^*.

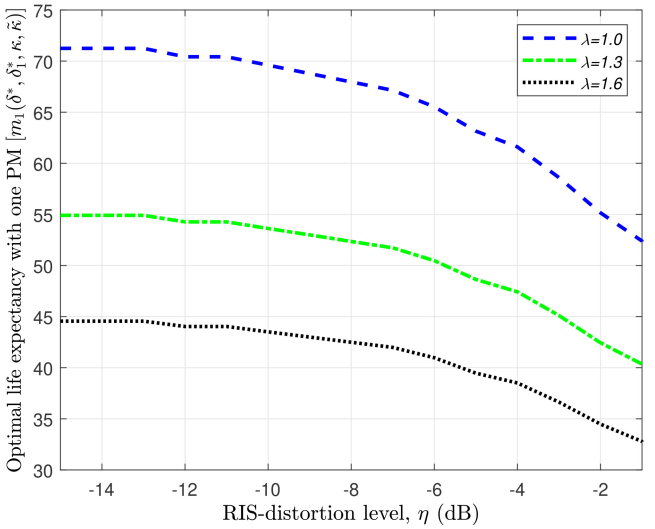

FIGURE 6. Optimal life extension versus observed distortion by the transmitter.

Hereinafter, we show the reliability analysis of the RIS-aided network in terms of BEP and BER, with respect to the RIS-distortion level. Here, we consider the binary PSK (BPSK) modulation scheme. Accordingly, by setting $M = 2$ and assigning $w = \pi/2$, the average BEP for the RIS-aided

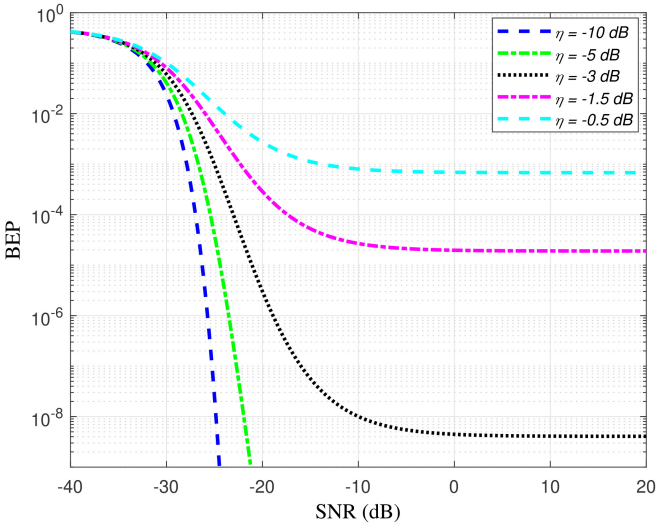

FIGURE 7. BEP performance for $N = 32$ and different values of η.

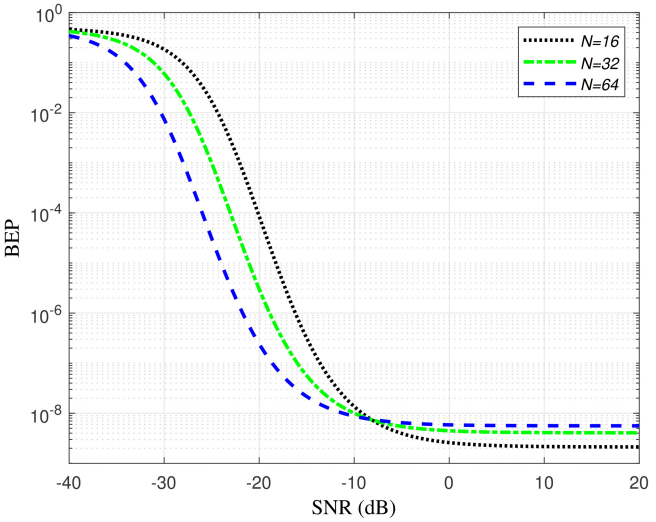

FIGURE 8. BEP performance for different numbers of RIS elements for $\eta = -3$dB.

system is upper-bounded as

$$\text{BEP}^{\text{BPSK}} \leq \frac{1}{2}\left(\frac{1}{1+2\text{Var}(\gamma_{\max})}\right)^{\frac{1}{2}} \exp\left[\frac{-4\left(\mathbb{E}[\gamma_{\max}]\right)^2}{1+2\text{Var}(\gamma_{\max})}\right]. \quad (35)$$

Here, we consider $N = 32$, and $P = 44$dBm. Fig. 7 shows the corresponding BEP for different levels of SNR[11] of the considered system with respect to varying RIS-distortion levels. It can be seen from the figure that, an increase in the level of RIS distortion leads to reduced BEP performance. The distortion is magnified in the high SNR regime, whereby it is observed that for higher distortion values ($\eta > -1.5$dB), the BEP curves saturate in the high SNR region. This is due to the fact that the BEP function decreases exponentially as the argument (in this case, SNR) increases. However, this decrease is not unlimited. The Q-function in Eq. (32) approaches a limit as its argument becomes very large. Mathematically, this limit can be expressed as: $\lim_{x\to 0} Q(x) = 0$. In this limit, as SNR becomes very high, the Q-function approaches zero, indicating that the BEP tends to zero. Hence, systematic maintenance must be performed to keep the value of η below the threshold to achieve a lower BEP. The RCF ensures this with the aid of statistical data, resulting in the RIS-aided transmission being more robust and less susceptible to estimation errors, which validates our proposed error analysis.

In Fig. 8, we show the BEP for different levels of SNR of the considered system with respect to varying RIS elements. Here, $\eta = -3$dB. In addition, to measure the actual rate at which bits are received incorrectly in the RIS-aided communication system the BER performance of the system with varying numbers of RIS elements is shown in Fig. 9. Here, the simulated BER is compared with the theoretical BER, i.e., $\frac{1}{2}\text{erfc}(\sqrt{P/N_0})$. It can be observed from the two figures that once the RCF has identified the RIS distortion level, the reliability of the network can be improved by increasing the number of RIS elements, which was already observed in Fig. 4. This result is a reflection of Proposition 4. The additional elements compensate for the misalignment of the impaired elements. By adjusting the phase of the new reflecting elements, the RIS directs the signal in the desired direction and achieves low BEP/BER and higher rates even in the low SNR regime.

[11]Here, we consider P/N_0 as the SNR, which is analogous to the conventional methods of diversity combining schemes.

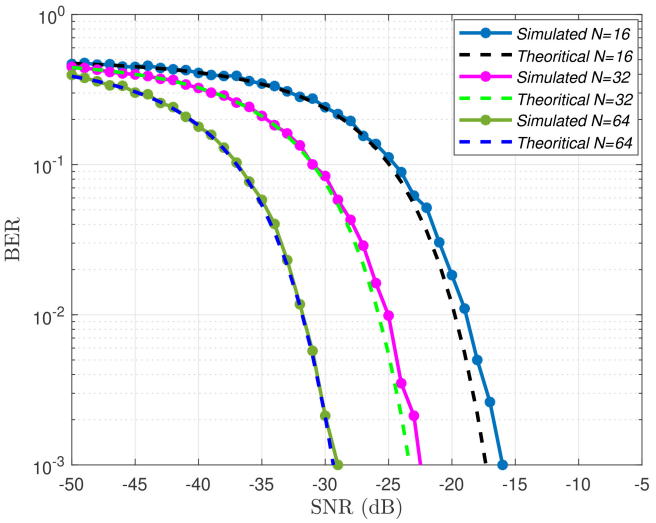

FIGURE 9. BER performance for different number of RIS elements for $\eta = -3$dB.

VII. CONCLUSION AND FUTURE WORK

We adopted an innovative approach to assess the hardware ageing effects of RIS-assisted IIoT communication systems with the goal of enhancing their longevity. This involved replicating diverse environments and simulating numerous scenarios to determine the optimal timing for

systematic maintenance, either immediately or as a postponement strategy, thereby extending the expected lifespan of the RIS system. Notably, the proposed EMF dynamically tailors interventions based on observed impairments and hardware constraints, providing the capability to optimize network performance and reliability. It was shown that the information-fused EMF framework can significantly extend the expected life cycle of a RIS system under the effect of non-residual hardware impairment by postponing maintenance. Furthermore, imperfect maintenance of the RIS elements was also considered, and accordingly, the communication reliability performance of the network was analyzed through the RCF with respect to BEP and BER. The proposed frameworks offer an economical means to assess performance, forecast the consequences of RIS-aided wireless network modifications, optimize network maintenance, and arrive at suitable decisions to prolong the life cycle of RISs.

In this work, the adoption of a simplified system model featuring a single antenna for both the transmitter and receiver was made to isolate the effects of RIS degradation and hardware impairments on the communication system's performance. This simplification allowed for the mathematical tractability of the proposed models. However, as part of our future work, we will extend this analysis to more complex system configurations, including multiple antennas and MIMO systems, to explore the interplay between RIS degradation and system architecture complexity. Another limitation of the current work is the non-inclusion of experimental results based on real-world data. Accordingly, in future, we intend to pursue the development of portable, cost-effective test-beds for simulating environmental stressors and their impacts on RIS hardware, which represents a promising avenue for bridging the gap between theoretical models and real-world operational dynamics. Furthermore, we also plan to explore RIS impairment models that account for non-uniform impairment levels, offering a more nuanced understanding of their impacts on system performance and maintenance strategies.

APPENDIX A
PROOF OF PROPOSITION 1

In order to show that (16) is unique, we have to show that the function $m_1(\delta,\kappa)$ is quasi-concave. Hence, we first find the Hessian of the function. Using Leibnitz rule, *i.e.,*

$$\frac{d}{d\kappa}\left(\int_u^v f(t)dt\right) = f(v)\frac{dv}{d\kappa} - f(u)\frac{du}{d\kappa}, \tag{A.1}$$

we first calculate the first order derivative of $m_1(\delta,\kappa)$ with respect to the time δ at which systematic maintenance of the RIS system is performed, *i.e.,* Accordingly, we have

$$\frac{dm_1(\delta,\kappa)}{d\delta} = \exp\{-\lambda\delta\}\sum_{i=0}^{N-1}\frac{(\lambda\delta)^i}{i!}\left(1+\frac{N}{\lambda}\right). \tag{A.2}$$

Now, assuming ζ_F as the Hessian of $m_1(\delta,\kappa)$, *i.e.,*

$$\begin{aligned}\zeta_F &= \frac{\partial^2 m_1(\delta,\kappa)}{\partial\delta^2},\\ &= (-2\lambda)\exp\{-\lambda\delta\}\sum_{i=0}^{N-1}\frac{(\lambda\delta)^i}{i!}\left(1+\frac{N}{\lambda}\right),\\ &= -2(\lambda+N)\exp\{-\lambda\delta\}\sum_{i=0}^{N-1}\frac{(\lambda\delta)^i}{i!}.\end{aligned}$$

The above implies that its Hessian is negative definite. As the parameter $\lambda > 0$ and N is a deterministic constant, we can conclude that,

$$\{\delta > 0 | \zeta_F \le 0\}.$$

This means that the expected mean lifetime $m_1(\delta,\kappa)$ of the RIS system is a concave function of δ.

Now, rewriting (A.2) as

$$\begin{aligned}m_1'(\delta,\kappa) &= -\bar{F}(\delta,\kappa)\lambda(\delta,\kappa)m(\kappa) + \bar{F}(\delta,\kappa),\\ &= \bar{F}(\delta,\kappa)(1-\lambda(\delta,\kappa)m(\kappa)),\end{aligned} \tag{A.3}$$

and equating it to zero, we have

$$\delta^* = \lambda^{-1}(1/m(\kappa),\kappa), \tag{A.4}$$

where $\lambda^{-1}(\cdot,\cdot)$ is the inverse function of $\lambda(\cdot,\cdot)$.

Let us consider $\lim_{t\to\infty}\lambda(t,\kappa) = \Lambda(\kappa) \le \infty$. When $\Lambda(\kappa) = \infty$, it implies that $\lim_{\delta\to\infty}\lambda(\delta,\kappa)m(\kappa) = \infty$, giving an optimal value of δ, i.e., δ^* at which $m_1(\delta,\kappa)$ achieves the maximum value and is denoted by $m_1(\delta^*,\kappa)$. Moreover, if $\Lambda(\kappa) < \infty$, it can be inferred from (A.3), that $\lim_{\delta\to\infty}\lambda(\delta,\kappa)m(\delta,\kappa) = 1$ implying $\lim_{\delta\to\infty}\lambda(\delta,\kappa)m(\kappa) > 1$ which is decreasing and therefore provides a unique solution to equation (16).

APPENDIX B
PROOF OF PROPOSITION 2

If multiple systematic maintenance are applied to the RIS system, *i.e.,* $n > 1$, the mean time to failure at $t = \delta_1$ can be expressed as

$$m_1(\delta_1,\kappa) = \int_0^{\delta_1}\bar{F}(t_{\tilde{\kappa}},\kappa)dt_{\tilde{\kappa}} + \bar{F}(\delta_1,\kappa)m(\kappa). \tag{B.1}$$

Now,

$$\begin{aligned}m_1(\delta_1,\delta_2;\kappa) &= \int_0^{\delta_1}\bar{F}(t_{\tilde{\kappa}},\kappa)dt_{\tilde{\kappa}} + \bar{F}(\delta_1,\kappa)\int_0^{\delta_2}\bar{F}(t_{\tilde{\kappa}},\kappa)dt_{\tilde{\kappa}}\\ &\quad + \bar{F}(\delta_1,\kappa)\bar{F}(\delta_2,\kappa)m(\kappa)\\ &= \int_0^{\delta_1}\bar{F}(t_{\tilde{\kappa}},\kappa)dt_{\tilde{\kappa}} + \bar{F}(\delta_1,\kappa)m_1(\delta_2,\kappa).\end{aligned} \tag{B.2}$$

Hence, for the inter-PM times, *i.e.,* δ_i $i = 1,2,\ldots,n$, the corresponding mean time to failure can be expressed as

$$\begin{aligned}&m_1(\delta_1,\delta_2,\ldots,\delta_n;\kappa)\\ &\quad= \int_0^{\delta_1}\bar{F}(t_{\tilde{\kappa}},\kappa)dt_{\tilde{\kappa}} + \bar{F}(\delta_1,\kappa)\int_0^{\delta_2}\bar{F}(t_{\tilde{\kappa}},\kappa)dt_{\tilde{\kappa}} + \ldots +\end{aligned}$$

$$\prod_{i=\delta}^{n-1}\bar{F}(\delta_i,\kappa)\int_0^{\delta_n}\bar{F}(t_{\tilde{\kappa}},\kappa)dt_{\tilde{\kappa}}+m(\kappa)\prod_{i=\delta}^{n}\bar{F}(\delta_i,\kappa)$$
$$=\int_0^{\delta_1}\bar{F}(t_{\tilde{\kappa}},\kappa)dt_{\tilde{\kappa}}+\bar{F}(\delta_1,\kappa)m_{n-1}(\delta_1,\delta_2,\ldots,\delta_n;\kappa). \tag{B.3}$$

As $m_n(0,0,\ldots,0)=m_n(\infty,\infty,\ldots,\infty)=m$, the optimal solution exists.

APPENDIX C
PROOF OF PROPOSITION 4

Consider $B=C\eta P+N_0$. Since $N\gg 1$, in accordance with the central limit theorem, the numerator term A in (28) follows a Gaussian distribution with mean and variance given as

$$\mathbb{E}[A]=\frac{N\pi}{4}\text{ and }\mathrm{Var}[A]=N\left(1-\frac{\pi^2}{16}\right),$$

respectively. Similarly, the mean and variance of the denominator term in (28) can be given as

$$\mathbb{E}[B]=\frac{N\pi}{4}\eta P+N_0\text{ and }\mathrm{Var}[B]=N\left(1-\frac{\pi^2}{16}\right)(\eta P)^2,$$

respectively. Now, the received SINR, *i.e.,* $\gamma_{\max}$ is in the form of a ratio. Hence, in accordance with the central limit theorem, $\gamma_{\max}$ also follows a Gaussian distribution. In addition, $\mathrm{cov}(A,B)\cong 0$ (refer Appendix E). Now, using Lemma 2 and after some mathematical manipulations, the desired expectation and variance of $\gamma_{\max}$ can be obtained.

APPENDIX D
PROOF OF PROPOSITION 5

Consider that $\gamma_{\max}$ follows a standard normal distribution with mean μ and variance σ. Considering that the MGF of $(\gamma_{\max}+\mu)^2$ exists, by definition, it can be written as

$$M_{\gamma_{\max}}(t)=\mathbb{E}\left[e^{t(\gamma+\mu)^2}\right]=\int_{-\infty}^{\infty}\mathrm{e}^{\mathrm{t}(\gamma+\mu)^2}\mathrm{f}_{\gamma_{\max}}(\gamma)\mathrm{d}\gamma, \tag{D.1}$$

where $f_{\gamma_{\max}}(\gamma)=\frac{1}{\sigma\sqrt{2\pi}}\mathrm{e}^{-\frac{1}{2}(\frac{\gamma-\mu}{\sigma})^2}$. Now, let $\frac{\gamma-\mu}{\sigma}=z$. Therefore,

$$M_{\gamma_{\max}}(t)=\frac{1}{\sigma\sqrt{2\pi}}\int_{-\infty}^{\infty}\mathrm{e}^{t(2\mu+\sigma z)^2}*\mathrm{e}^{-\frac{z^2}{2}}\sigma dz$$
$$=\frac{1}{\sqrt{2\pi}}\int_{-\infty}^{\infty}\exp\left[-\left(\frac{1}{2}-\sigma^2t\right)z^2+4\mu\sigma zt+4\mu^2t\right]dz. \tag{D.2}$$

Now, by writing $Q=\frac{4\mu\sigma t}{1-2\sigma^2t}$, we have

$$M_{\gamma_{\max}}(t)=\frac{1}{\sqrt{2\pi}}\int_{-\infty}^{\infty}\exp\left[-\left(\frac{1}{2}-\sigma^2t\right)(z-Q)^2+4\mu^2t+\frac{8\mu^2\sigma^2t^2}{1-2\sigma^2t}\right]dz,$$
$$=\exp\left[\frac{4\mu^2t}{1-2\sigma^2t}\right]\left(1-2\sigma^2t\right)^{-\frac{1}{2}}\times$$
$$\frac{1}{\sqrt{2\pi}\left(1-2\sigma^2t\right)^{-\frac{1}{2}}}\int_{-\infty}^{\infty}\exp\left[-\frac{(z-Q)^2}{2\left(1-2\sigma^2t\right)^{-1}}\right]dz. \tag{D.3}$$

Solving (D.3), we can obtain the MGF as

$$M_{\gamma_{\max}}(t)=\left(\frac{1}{1-2\sigma^2t}\right)^{\frac{1}{2}}\exp\left[\frac{4\mu^2t}{1-2\sigma^2t}\right].$$

Substituting, the values of μ and σ from (29) and (30), respectively we obtain the desired proof.

APPENDIX E

From the properties of covariance, we have

$$\mathrm{cov}(XY)=\mathbb{E}(XY)-\mathbb{E}(X)\mathbb{E}(Y) \tag{E.1}$$

In reference to (28), consider $X=(\sum_{i=1}^{N}\alpha_i\beta_i)^2P$ and $Y=(\sum_{i=1}^{N}\alpha_i\beta_i)^2\eta P+N_0$. As we already know, $\mathbb{E}[\alpha_i\beta_i]=\frac{\pi}{4}$, therefore $\mathbb{E}(X)=\frac{N\pi}{4}P$ and $\mathbb{E}(Y)=\frac{N\pi}{4}\eta P+N_0$.

Now,

$$\mathbb{E}(X)\mathbb{E}(Y)=\frac{N\pi}{4}P\left[\frac{N\pi}{4}\eta P+N_0\right],$$
$$=\left(\frac{N\pi}{4}\right)^2\eta P^2+\left(\frac{N\pi}{4}\right)N_0P. \tag{E.2}$$

Again,

$$\mathbb{E}(XY)=\mathbb{E}\left[\left(\sum_{i=1}^{N}\alpha_i\beta_i\right)^2P\left\{\left(\sum_{i=1}^{N}\alpha_i\beta_i\right)^2\eta P+N_0\right\}\right],$$
$$=\mathbb{E}\left[\left(\sum_{i=1}^{N}\alpha_i\beta_i\right)^4\eta P^2+\left(\sum_{i=1}^{N}\alpha_i\beta_i\right)^2PN_0\right],$$
$$=\mathbb{E}\left[\left(\sum_{i=1}^{N}\alpha_i\beta_i\right)^4\eta P^2\right]+\mathbb{E}\left[\left(\sum_{i=1}^{N}\alpha_i\beta_i\right)^2PN_0\right],$$
$$=\left(\frac{N\pi}{4}\right)^2\eta P^2+\left(\frac{N\pi}{4}\right)N_0P. \tag{E.3}$$

Using (E.2) and (E.3) in (E.1), we get $\mathrm{cov(XY)}=0$. Therefore, we can infer that the random variable X and Y are independent.

REFERENCES

[1] P. Wang, J. Liu, G. Huang, Q. Wu, C. Zhou, and W. Wang, "Wideband gain enhancement of high-isolation and quasi-omnidirectional metamaterial MIMO antenna for vehicular radar," *IEEE Trans. Instrum. Meas.*, vol. 71, pp. 1–12, Sep. 2022.

[2] R. Rodriguez-Cano, S. E. Perini, B. M. Foley, and M. Lanagan, "Broadband characterization of silicate materials for potential 5G/6G applications," *IEEE Trans. Instrum. Meas.*, vol. 72, pp. 1–8, Mar. 2023.

[3] Q. Wu and R. Zhang, "Towards smart and reconfigurable environment: Intelligent reflecting surface aided wireless network," *IEEE Commun. Mag.*, vol. 58, no. 1, pp. 106–112, Jan. 2020.

[4] C. Huang et al., "Holographic MIMO surfaces for 6G wireless networks: Opportunities, challenges, and trends," *IEEE Wireless Commun.*, vol. 27, no. 5, pp. 118–125, Oct. 2020.

[5] I. F. Akyildiz, A. Kak, and S. Nie, "6G and beyond: The future of wireless communications systems," *IEEE Access*, vol. 8, pp. 133995–134030, 2020.

[6] M. Poulakis, "6G's metamaterials solution: There's plenty of bandwidth available if we use reconfigurable intelligent surfaces," *IEEE Spectr.*, vol. 59, no. 11, pp. 40–45, Nov. 2022.
[7] N. H. Mahmood, G. Berardinelli, E. J. Khatib, R. Hashemi, C. De Lima, and M. Latva-aho, "A functional architecture for 6G special-purpose Industrial IoT networks," *IEEE Trans. Ind. Informat.*, vol. 19, no. 3, pp. 2530–2540, Mar. 2023.
[8] S. Li et al., "Orthogonal chirp division multiplexing assisted dual-function radar communication in IoT networks," *IEEE Internet Things J.*, early access, Apr. 9, 2024, doi: 10.1109/JIOT.2024.3386666.
[9] C. Pan et al., "Reconfigurable intelligent surfaces for 6G systems: Principles, applications, and research directions," *IEEE Commun. Mag.*, vol. 59, no. 6, pp. 14–20, Jun. 2021.
[10] E. Björnson, Ö. Özdogan, and E. G. Larsson, "Reconfigurable intelligent surfaces: Three myths and two critical questions," *IEEE Commun. Mag.*, vol. 58, no. 12, pp. 90–96, Dec. 2020.
[11] J. Zhang, Z. Zheng, Z. Fei, and Z. Han, "Energy-efficient multiuser localization in the RIS-assisted IoT networks," *IEEE Internet Things J.*, vol. 9, no. 20, pp. 20651–20665, Oct. 2022.
[12] J. Zhang, J. Wu, and R. Wang, "User localization and environment mapping with the assistance of RIS," *IEEE Trans. Veh. Technol.*, early access, Feb. 2, 2024, doi: 10.1109/TVT.2024.3361475.
[13] C. Molero et al., "Metamaterial-based reconfigurable intelligent surface: 3D meta-atoms controlled by grapheme structures," *IEEE Commun. Mag.*, vol. 59, no. 6, pp. 42–48, Jun. 2021.
[14] L. Dai et al., "Reconfigurable intelligent surface-based wireless communications: Antenna design, prototyping, and experimental results," *IEEE Access*, vol. 8, pp. 45913–45923, 2020.
[15] M. Di Renzo et al., "Smart radio environments empowered by reconfigurable intelligent surfaces: How it works, state of research, and the road ahead," *IEEE J. Sel. Areas Commun.*, vol. 38, no. 11, pp. 2450–2525, Nov. 2020.
[16] X. Yuan, Y.-J. A. Zhang, Y. Shi, W. Yan, and H. Liu, "Reconfigurable-intelligent-surface empowered wireless communications: Challenges and opportunities," *IEEE Wireless Commun.*, vol. 28, no. 2, pp. 136–143, Apr. 2021.
[17] Q. Ni, J. C. Ji, and K. Feng, "Data-driven prognostic scheme for bearings based on a novel health indicator and gated recurrent unit network," *IEEE Trans. Ind. Informat.*, vol. 19, no. 2, pp. 1301–1311, Feb. 2023.
[18] M. Finkelstein and J. H. Cha, "Reducing degradation and age of items in imperfect repair modeling," *Test*, vol. 31, no. 4, pp. 1058–1081, 2022.
[19] J. H. Cha and M. Finkelstein, "On optimal life extension for degrading systems," *Proc. Inst. Mech. Eng., Part O, J. Risk Rel.*, vol. 234, no. 3, pp. 487–495, 2020.
[20] A. Mondal, A. M. A. Junaedi, K. Singh, and S. Biswas, "Spectrum and energy-efficiency maximization in RIS-aided IoT networks," *IEEE Access*, vol. 10, pp. 103538–103551, 2022.
[21] K. Singh, P.-C. Wang, S. Biswas, S. K. Singh, S. Mumtaz, and C.-P. Li, "Joint active and passive beamforming design for RIS-aided IBFD IoT communications: QoS and power efficiency considerations," *IEEE Trans. Consum. Electron.*, vol. 69, no. 2, pp. 170–182, May 2023.
[22] S. Lin, Y. Zou, B. Li, and T. Wu, "Security-reliability trade-off analysis of RIS-aided multiuser communications," *IEEE Trans. Veh. Technol.*, vol. 72, no. 5, pp. 6225–6237, May 2023.
[23] Z. Chu et al., "RIS assisted wireless powered IoT networks with phase shift error and transceiver hardware impairment," *IEEE Trans. Commun.*, vol. 70, no. 7, pp. 4910–4924, Jul. 2022.
[24] H. Zheng et al., "Robust transmission design for RIS-aided wireless communication with both imperfect CSI and transceiver hardware impairments," *IEEE Internet Things J.*, vol. 10, no. 5, pp. 4621–4635, Mar. 2023.
[25] L. Qu, C. Assi, K. Shaban, and M. J. Khabbaz, "A reliability-aware network service chain provisioning with delay guarantees in NFV-enabled enterprise datacenter networks," *IEEE Trans. Netw. Service Manag.*, vol. 14, no. 3, pp. 554–568, Sep. 2017.
[26] Y. Wu, W. Zheng, Y. Zhang, and J. Li, "Reliability-aware VNF placement using a probability-based approach," *IEEE Trans. Netw. Service Manag.*, vol. 18, no. 3, pp. 2478–2491, Sep. 2021.
[27] M. Finkelstein, J. H. Cha, and S. Ghosh, "Optimal inspection for missions with a possibility of abortion or switching to a lighter regime," *Top*, vol. 29, pp. 722–740, Jan. 2021.
[28] H. Taghvaee, A. Cabellos-Aparicio, J. Georgiou, and S. Abadal, "Error analysis of programmable metasurfaces for beam steering," *IEEE J. Emerg. Select. Topics Circuits Syst.*, vol. 10, no. 1, pp. 62–74, Mar. 2020.
[29] H. Taghvaee, S. Abadal, J. Georgiou, A. Cabellos-Aparicio, and E. Alarcón, "Fault tolerance in programmable metasurfaces: The beam steering case," in *Proc. IEEE Int. Symp. Circuits Syst. (ISCAS)*, 2019, pp. 1–5.
[30] S. Zhao, V. Makis, S. Chen, and Y. Li, "Health assessment method for electronic components subject to condition monitoring and hard failure," *IEEE Trans. Instrum. Meas.*, vol. 68, no. 1, pp. 138–150, Jan. 2019.
[31] S. Zhao, S. Chen, and H. Wang, "Degradation modeling for reliability estimation of DC film capacitors subject to humidity acceleration," *Microelectron. Rel.*, vols. 100–101, Sep. 2019, Art. no. 113401.
[32] C. Öztürk, M. F. Keskin, H. Wymeersch, and S. Gezici, "On the impact of hardware impairments on RIS-aided localization," in *Proc. IEEE Int. Conf. Commun.*, 2022, pp. 2846–2851.
[33] F. Ghaseminajm, M. Alsmadi, D. Tubail, and S. S. Ikki, "RIS-aided mobile localization error bounds under hardware impairments," *IEEE Trans. Commun.*, vol. 70, no. 12, pp. 8331–8341, Dec. 2022.
[34] Y. Lu, J. Zhang, J. Zheng, H. Xiao, and B. Ai, "Performance analysis of RIS-assisted communications with hardware impairments and channel aging," *IEEE Trans. Commun.*, early access, Feb. 2, 2024, doi: 10.1109/TCOMM.2024.3361554.
[35] W. Namgoong, "Modeling and analysis of nonlinearities and mismatches in AC-coupled direct-conversion receiver," *IEEE Trans. Wireless Commun.*, vol. 4, no. 1, pp. 163–173, Jan. 2005.
[36] H. Suzuki, T. V. A. Tran, I. B. Collings, G. Daniels, and M. Hedley, "Transmitter noise effect on the performance of a MIMO-OFDM hardware implementation achieving improved coverage," *IEEE J. Sel. Areas Commun.*, vol. 26, no. 6, pp. 867–876, Aug. 2008.
[37] J. Craig, "A new, simple and exact result for calculating the probability of error for two-dimensional signal constellations," in *Proc. Conf. Rec.*, 1991, pp. 571–575.
[38] D. Goyal, N. K. Hazra, and M. Finkelstein, "On the time-dependent delta-shock model governed by the generalized Pólya process," *Methodol. Comput. Appl. Probab.*, vol. 24, pp. 1627–1650, Sep. 2022.

ATIQUZZAMAN MONDAL received the B.Tech. and M.Tech. degrees in electronics and communication engineering from North Eastern Hill University, Shillong, India, in 2015 and 2017, respectively. He is currently pursuing the Ph.D. degree in 6G wireless communication with the Indian Institute of Information Technology Guwahati, India. He also worked on a project funded by Science and Engineering Research Board. His research interests include reconfigurable intelligent surface-aided wireless communications, full-duplex radio, optimization, and NTN for communications.

SHYAMAL GHOSH (Member, IEEE) received the M.Sc. degree in applied mathematics and the Ph.D. degree in applied probability and statistics from the Indian Institute of Engineering Science and Technology, Shibpur, India, in 2014 and 2019, respectively. He is currently an Assistant Professor with the School of Data Science, Indian Institute of Information Science Education and Research, Thiruvananthapuram, India. His research interests include reliability theory, stochastic degradation modeling, dependence modeling, statistical inference, and applied probability. He is a Lifetime Member of the International Indian Statistical Association.

KESHAV SINGH (Member, IEEE) received the Ph.D. degree in communication engineering from National Central University, Taiwan, in 2015. He is currently works as an Assistant Professor with the Institute of Communications Engineering, National Sun Yat-sen University, Taiwan. Prior to this, he held the position of Research Associate with the Institute of Digital Communications, University of Edinburgh, U.K., from 2016 to 2019. From 2019 to 2020, he was associated as a Research Fellow with the University College Dublin, Ireland. He chaired workshops on conferences like IEEE GLOBECOM 2023 and IEEE WCNC, 2024. He also serves as a Leading Guest Editor for the IEEE TRANSACTIONS ON GREEN COMMUNICATIONS AND NETWORKING Special Issue on Design of Green Near-Field Wireless Communication Networks. He leads research in the areas of green communications, resource allocation, transceiver design for full-duplex radio, ultra-reliable low-latency communication, non-orthogonal multiple access, machine learning for wireless communications, integrated sensing and communications, non-terrestrial networks, and large intelligent surface-assisted communications.

SUDIP BISWAS (Member, IEEE) received the Ph.D. degree in digital communications from the University of Edinburgh (UEDIN), U.K., in 2017.

He currently works as an Associate Professor with the Department of Electronics and Communications Engineering, Indian Institute of Information Technology Guwahati. From 2017 to 2019, he was a Research Associate with the Institute of Digital Communications, UEDIN. He also has industrial experience with Tata Consultancy Services, Lucknow and Kolkata, India, where he was an Assistant Systems Engineer, from 2010 to 2012. He has published more than 70 technical papers in reputed international journals and conferences and has been involved in EU FP7 projects: remote radio heads and parasitic antenna arrays and dynamic licensed shared access, a DST UKIERI project on wireless edge caching, and an EPSRC project on NoMA. He has received several research grants on various topics in signal processing, machine learning and IoT from various government funding agencies with an accumulated research funding of more than 2M$. He is currently leading four DST-funded projects as PI and two projects as Co-PI. He leads research on signal processing and machine learning for wireless communications, with particular focus on 6G communications. He is an Editor of IEEE TRANSACTIONS ON GREEN COMMUNICATIONS.

TRUNG Q. DUONG (Fellow, IEEE) is a Canada Excellence Research Chair and a Full Professor with the Memorial University of Newfoundland, Canada, an Adjunct Chair Professor in telecommunications with Queen's University Belfast, U.K., and a Research Chair of Royal Academy of Engineering, U.K. His current research interests include quantum communications, wireless communications, quantum machine learning, and quantum optimization.

Dr. Duong received the Best Paper Award at the IEEE VTC-Spring 2013, IEEE ICC 2014, IEEE GLOBECOM 2016, 2019, and 2022, IEEE DSP 2017, IWCMC 2019 and 2023, and IEEE CAMAD 2023. He has received the two prestigious awards from the Royal Academy of Engineering (RAEng): RAEng Research Chair from 2021 to 2025 and the RAEng Research Fellow from 2015 to 2020. He is the recipient of the prestigious Newton Prize 2017. He has served as an Editor/Guest Editor for the IEEE TRANSACTIONS ON WIRELESS COMMUNICATIONS, the IEEE TRANSACTIONS ON COMMUNICATIONS, the IEEE TRANSACTIONS ON VEHICULAR TECHNOLOGY, IEEE COMMUNICATIONS LETTERS, IEEE WIRELESS COMMUNICATIONS LETTERS, IEEE WIRELESS COMMUNICATIONS, IEEE COMMUNICATIONS MAGAZINES, and IEEE JOURNAL ON SELECTED AREAS IN COMMUNICATIONS.